Available online at www.sciencedirect.com
ScienceDirect
Journal of Power Sources 160 (2006) 440–445
JOURNAL OF POWER SOURCES
www.elsevier.com/locate/jpowsour

Determination of DMFC deterioration during long-term operation

Ho Kim [a,*], Se-Jong Shin [a], Young-gil Park [a], Joohan Song [a], Hee-tak Kim [b]

[a] *Analysis Team, Corporate R&D center, Samsung SDI Co., Ltd., Giheung 449-902, Yong-in, Republic of Korea*
[b] *Energy Lab., Corporate R&D center, Samsung SDI Co., Ltd., Shin-dong 443-731, Suwon, Republic of Korea*

Received 29 October 2005; received in revised form 22 December 2005; accepted 22 December 2005
Available online 23 February 2006

Abstract

A new method to analyze deteriorated direct methanol fuel cells (DMFCs) by combining electrochemical impedance analysis and physicochemical investigations is proposed. To make a comparison, one pristine membrane electrode assembly (MEA) and one deteriorated MEA, following 1000 h of continuous operation, were prepared. A unique impedance analysis enabled the separation of the impedance values for the cathode and the anode, and it was possible to determine that the deterioration of the MEA mainly came from the deterioration of the cathode. Several physicochemical investigations were made to show the relationship between the electrochemical properties and the deterioration of the MEA.

Keywords: Direct methanol fuel cell; Deterioration; Long-term operation; Impedance

1. Introduction

Direct methanol fuel cells (DMFCs) have been attractive electrochemical devices for consideration in transportation and portable applications as they offer many advantages, such as elimination of fuel reforming, ease in refueling and a simplified system design [1–3]. However, a number of significant technical problems must be resolved, although recent development efforts have successfully overcome many of the existing barriers to the practical implementation of the fuel cells. One has to offer a fuel cell system that supplies high performances for the required lifetime before DMFCs can be commercialized. Fuel cell lifetime requirements vary significantly, ranging from 3000 to 5000 operating hours for car applications and up to 20,000 operating hours for bus applications and up to 40,000 operating hours for stationary applications [1]. Yet, current DMFCs are still having difficulty in reaching these goals, since various deteriorations and degradations impact the durability and efficiency during the long-term operations.

To date, many investigations have been made to find the mechanisms of fuel cell deterioration using various techniques. Schulze et al. reported alteration of the platinum distribution and a migration of platinum after operation [4] and Blom et al. showed the catalyst agglomeration after operation from TEM examination [5]. Lim and Wang [2] and other researchers [6–8] investigated the causes of deterioration due to changes in transportation within the gas diffusion layers (GDLs) and the micro porous layers (MPLs). On the other hand, some researchers, such as, Lee et al. [9] and Romero-Castanon et al. [10], and Mueller and Urban [11] applied electrochemical impedance spectroscopy as a tool in MEA evaluation.

In this paper, we suggest a new method to evaluate MEA degradation by a combination of electrochemical impedance analysis and physicochemical investigation.

One MEA was deliberately degraded by operating for 1000 h continuously, and we confirmed the alteration of impedance compared to an MEA which had not been through the same operation.

In particular, we evaluated the electrochemical impedance of the cathode and anode separately, and as a result, we were able to point out that cathode deterioration was the main cause of loss of MEA performance. In order to confirm this deterioration phenomena between the cathode and anode, we collected physicochemical evidence by applying field emission-scanning electron microscopy and energy dispersive X-ray spectroscopy (FE-SEM/EDS), drop shape analysis (DSA), X-ray photoelectron spectroscopy (XPS), field emission-transmission electron microscopy (FE-TEM) to the MEAs.

* Corresponding author. Tel.: +82 31 288 4358; fax: +82 54 288 4304.
E-mail address: ho312.kim@samsung.com (H. Kim).

0378-7753/$ – see front matter © 2006 Elsevier B.V. All rights reserved.
doi:10.1016/j.jpowsour.2005.12.057

2. Experimental

2.1. MEA preparation and long-term operation

MEAs were prepared with the same materials and manufacturing protocols. For membranes, commercial Nafion 115 (DuPont, USA) were used. Twenty weight percent PTFE treated SGL 10EA carbon papers (from SGL carbon, Germany) were used for the cathode GDLs, while non-PTFE treated SGL 10AA carbon papers (from SGL carbon) were used for the anode GDLs. To fabricate MPLs, each carbon paper was spray-coated with a solution comprising 50 wt.% Vulcan XC-72 carbon (from Cabot, USA) in PTFE solution. In the case of the catalyst layers, commercially available Pt-black (HiSPEC 1000, Johnson Matthey, USA) for cathodes, and Pt/Ru-black (HiSPEC 6000, Johnson Matthey) for the anodes were suspended in 5 wt.% Nafion solutions, and spray-coated onto each side of MPLs to give the approximate loading of 6.9 mg cm^{-2} of Pt-black on cathodes and 7.9 mg cm^{-2} of Pt/Ru-black on anodes, respectively. After trimming the catalyzed electrodes for the anodes and cathodes, they were positioned on both sides of the pre-cleaned Nafion 115 membrane and hot-pressed to form a unit of MEA at 125 °C for 3 min.

Then, for the 1000 h continuous operation, an MEA was inserted into a single cell fixture (consisting of graphite plates with an active area of 10 cm^2, Amitech, Korea) having two-pass serpentine flow channels on each side of the electrodes, respectively. The decay of output voltage and current density were monitored while the MEA was operated continuously by feeding a diluted 1 M methanol solution at the constant current load of 1.6 A and the operational temperature of 50 °C.

2.2. Electrochemical impedance analysis

Electrochemical impedance was measured under galvanostatic control. The amplitude of the sinusoidal voltage signal was set to 5 mV. To get information on the electrochemical reactions at the electrodes, MEAs were operated to generate 90 mA cm^{-2} under total impedance measurement at air per 1 M MeOH feed. We also measured anode impedances in order to separate anode and cathode impedances from the total impedance. For anode impedance measurements, the cathode feed was replaced with hydrogen [11]. By subtracting the anode impedances

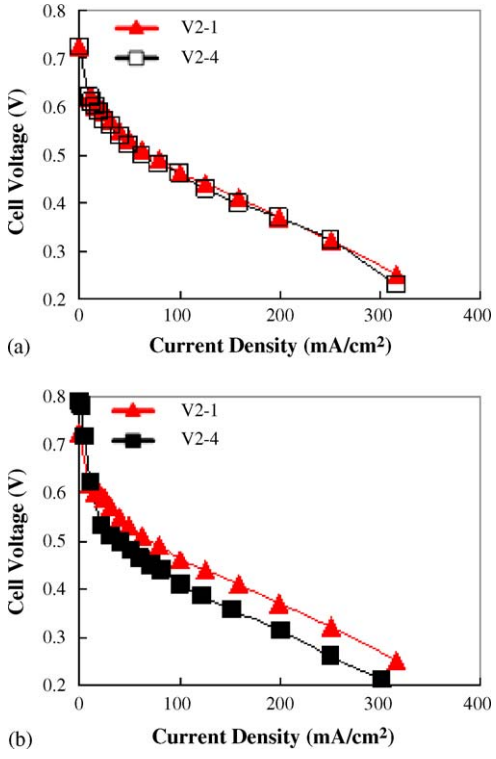

Fig. 1. A comparison of MEA performances: (a) polarizations of V2-1 and V2-4 right after the activation process and (b) polarizations of V2-1 and V2-4 after the 1000-h continuous operation of V2-4.

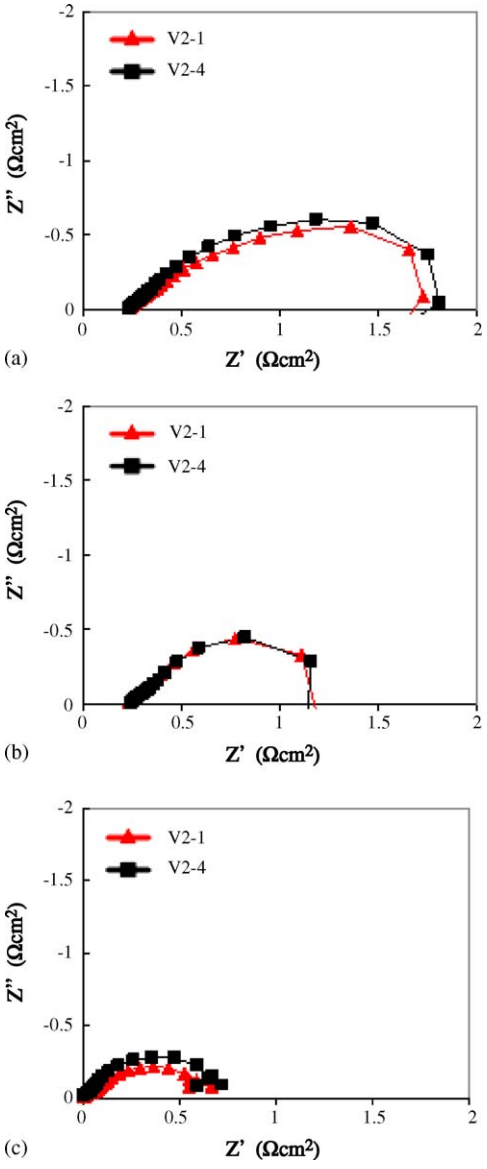

Fig. 2. A comparison of Nyquist plots of: (a) total impedance, (b) anode impedance and (c) cathode impedance of MEAs V2-1 and V2-4, respectively.

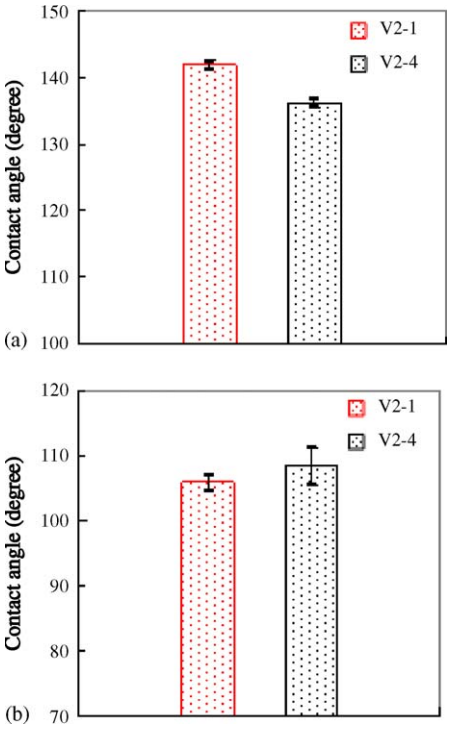

Fig. 3. A comparison of contact angles of (a) cathode side GDLs and (b) anode side GDLs of MEAs V2-1 and V2-4 after the operation of V2-4. Values are averages of three data points on each sample, respectively. Anode side GDLs showed large variation during the measurements.

from the total impedances, the cathode impedances were extracted.

2.3. Physicochemical investigations

Possible degradations of the GDLs and MPLs were investigated with a FE-SEM (JSM-6700F, Jeol, Japan) and DSA (DSA10 Mk2, Kruss, Germany). And, for the catalyst layers, FE-SEM/EDS (Oxford Instruments Inc., England) and XPS (ESCALAB 250, VG Scientific, England), FE-TEM (G2 F30 S-TWIN, Tecnai, Holland) were used for comparison.

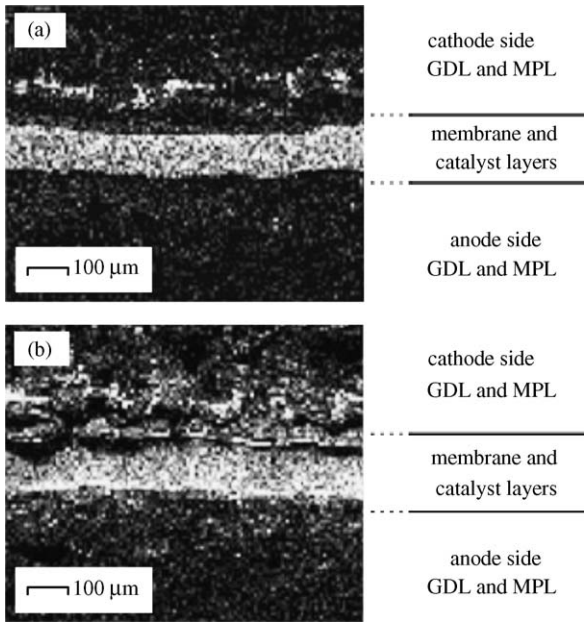

Fig. 5. A comparison of cross-sectional FE-SEM/EDS mapping images on fluorine content: (a) V2-1 and (b) V2-4 after the operation. White areas indicate the existence of fluorine contents.

3. Results and discussion

3.1. Deterioration of the MEA

To have MEAs compared by dismantling, two MEAs had to be selected prior to the operation. 'V2-1' and 'V2-4' were chosen among MEAs, since those showed similar *I–V* characteristics during the operation as shown in Fig. 1a. Though the *I–V* characteristics were not thought to be enough to prove that the two MEAs were exactly the same, they were thought enough to be compared to show physicochemical changes from long-term operation.

Between them, V2-4 was operated continuously while the decay of the output voltage and current density were monitored. On the other hand, V2-1 was kept under an inert environment to maintain the original condition.

Fig. 1b illustrates the polarization curves for both MEAs after operation of V2-4. Performance loss occurred at low current

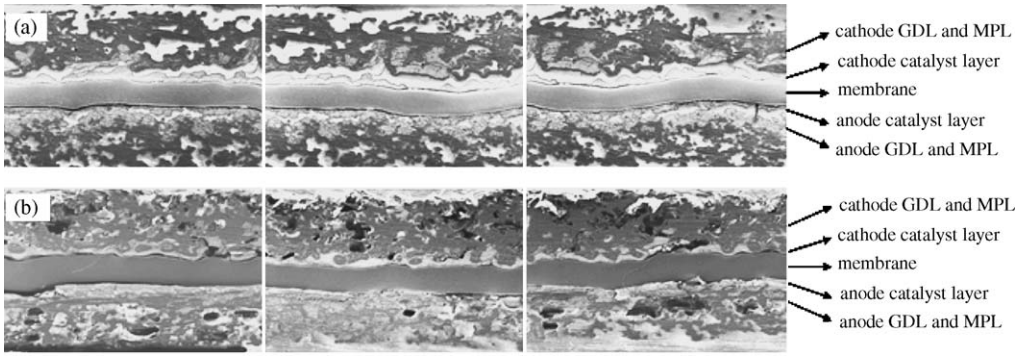

Fig. 4. A comparison of cross-sectional FE-SEM images: (a) V2-1 and (b) V2-4 after the operation.

density, and the extent of this loss became greater in the high current density region for V2-4. Increased resistance on mass transport and a decreased catalytic efficiency were thought to be responsible.

3.2. Electrochemical impedance analysis

As mentioned above, it has been noticed that changes in the electrochemical impedance are good indicators of the condition of MEAs [9–11].

Fig. 2 shows the impedance changes under long-term operation. In Fig. 2a, the semi-circle that corresponds to the contribution from the electrochemical reaction at the anode and the cathode became larger after long-term operation, which indicates the electrochemical reaction rate decreased after this operation. Interestingly, the anode impedance did not show significant changes, however, a profound increase in the cathode impedance was observed as shown in Fig. 2b and c. It strongly suggests that the decrease of power density following operation (Fig. 1b) mainly comes from the deterioration of the cathode. Therefore, in the following subsections, physicochemical investigations are described to determine the reasons responsible for the deterioration of the cathode.

3.3. Deterioration of the cathode

As many researchers have suggested, increase of resistance to mass transport mainly occurs when the MEAs fail in their water management [2,6–8]. Therefore, the early stage of the investigations was focused on comparing the water management capabilities of V2-1 and V2-4, and revealing the cathode deterioration of 1000 h-operated V2-4.

Fig. 3 shows the values of the contact angles measured by DSA in the outer layers of the MEAs. The values are averages of three repeated experiments for each electrode. In Fig. 3a, a minor decrease of contact angle was found on the cathode side of V2-4. This 5° difference of contact angle might have caused a small increase in mass transport resistance, but was still not

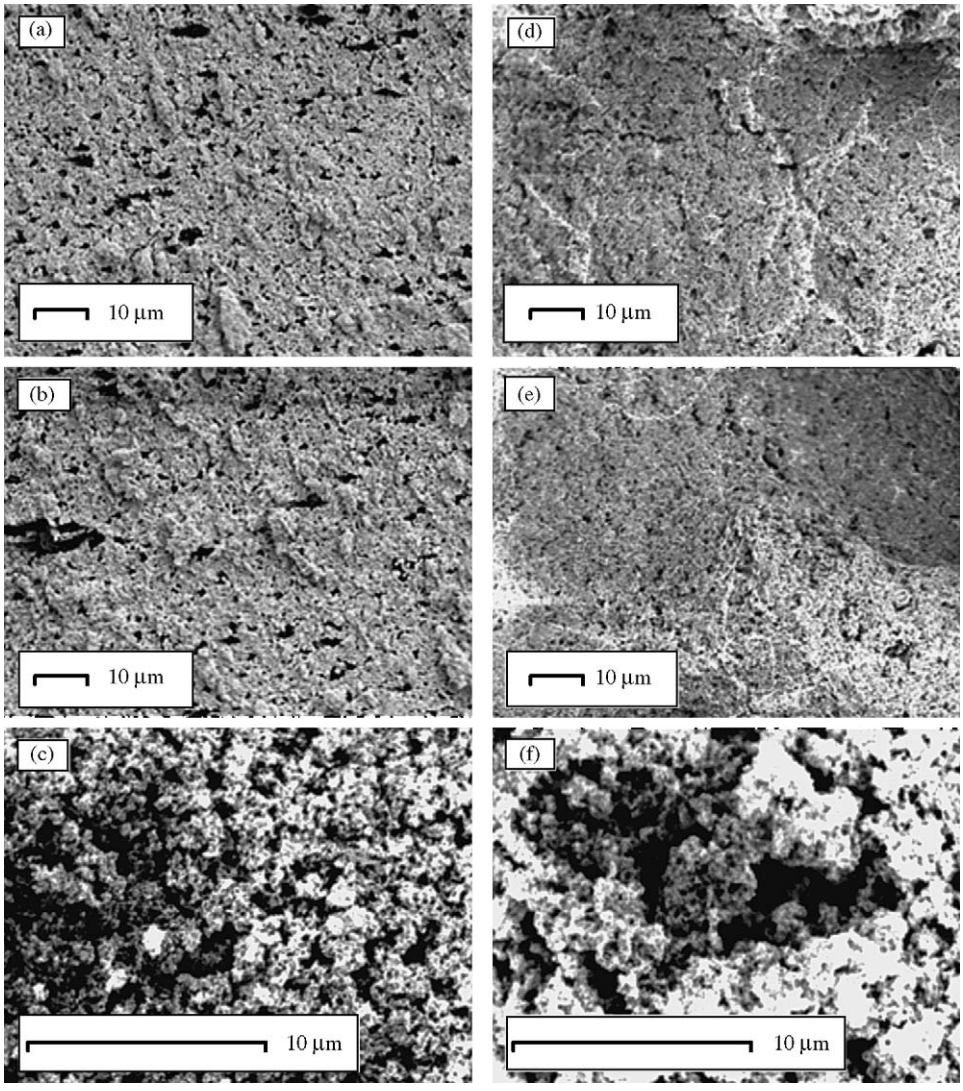

Fig. 6. SEM surface micrographs of the cathode side catalyst layers: (a and b) V2-1 of 1000 magnifications, (c) V2-1 of 5000 magnification, (d and e) V2-4 of 1000 magnifications and (f) V2-4 of 5000 magnification.

enough to explain the impedance increment. In the case of the anode, on the other hand, a difference was not found as shown in Fig. 3b.

A cross-sectional FE-SEM investigation was performed to compare the morphologies of the GDLs and MPLs. Fig. 4 shows the cross-sectional micrographs of the MEAs, which were hardened by Caldofix resin (Struers, Denmark) and cross-sectioned to avoid breakage during the pre-treatment. Bright white areas indicated in both Fig. 4a and b correspond to the resin areas, and the areas also represented pores, which existed before hardening. The pores in GDLs and MPLs should be maintained properly for water management and sufficient fuel supply. However, by simply comparing the pores, a decrease of mass transport and increase of resistance were suspected to be due to the decrease of pores on the cathode side.

In terms of water management, Lim and Wang suggested that the amount of water proofing agent in the GDLs controls the MEA performance [2]. However, FE-SEM/EDS mapping images of the fluorinated water proofing agents (Fig. 5) suggested that a diffusion and redistribution of the water proofing agents in the GDLs and MPLs became critical in water management. Comparison of Fig. 5a and b show that the fluorine content was disproportional and gathered on cathode side of the GDL and MPL. Therefore, it was thought that the uneven distribution of the water proofing agent made newly generated water molecules on cathode side difficult to be ejected through the GDLs, and also increased the impedance of the cathode.

Catalyst layers were sectioned and surface morphologies were compared by FE-SEM. In Fig. 6, the surface of the catalyst layers are shown for two magnifications of each MEA. Fig. 6a–c correspond to V2-1 and Fig. 6d–f correspond to V2-4 MEA. From the figures, an increase in the mass transport resistance of the catalyst layers is suspected from the changes in the outward appearance of the closely packed catalyst layers after prolonged operation. Summarizing the data collected so far, it suggests that the decrease of pores in GDLs and MPLs, dense catalyst layers, and the redistribution of the water proofing agent might interact to affect the mass transport and electrochemical impedance.

In terms of catalyst deterioration on the cathode, agglomerations and chemical state changes were found by TE-TEM and XPS. Fig. 7 illustrates the agglomeration and size distribution of catalysts by measuring 40 catalyst grains of each MEA. In Fig. 7a, the diameter of the V2-1 catalysts was about 5 nm on average. But after the prolonged operation of V2-4, the size increased to 8 nm as indicated in Fig. 7b. Fig. 7c indicates the numbers of particles counted and measured by averaging the size of the catalysts. From the bar graph of Fig. 7c, the size distribution of the cathode catalyst seemed to be increased for V2-4. This kind of agglomeration is believed to decrease the reaction surface of the catalyst, and in the end, cause performance loss of the MEA.

As mentioned above, XPS analysis showed chemical state changes, a reduction of the platinum catalysts, as illustrated in Fig. 8a. It was known that the peaks of Pt 4f7/2 with binding energies higher than 72 eV are related to the oxide forms of Pt [12–15]. In Fig. 8a, however, the peaks around 72 eV were

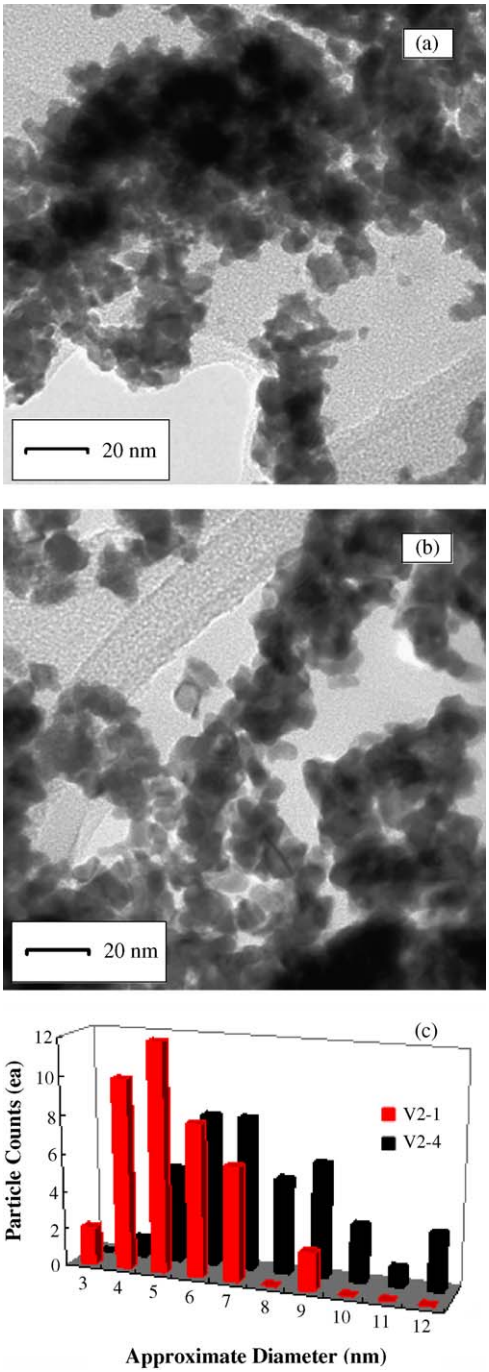

Fig. 7. A comparison of TEM micrographs and size distribution of the cathode catalysts: (a) V2-1, (b) V2-4 after the operation and (c) catalyst size distribution of V2-1 and V2-4 after the operation.

decreased and metallic form of Pt (approximately 71 eV) became dominant after prolonged operation (a black colored line in the figure). This change was confirmed by repeating the experiments seven times on random points. Chemical reduction of platinum is a small but nevertheless an important change, since the chemical state distribution is believed to affect the catalytic efficiency during prolonged operation.

However, compared to the changes of the cathode side, there was no change in the catalyst composition and chemical states

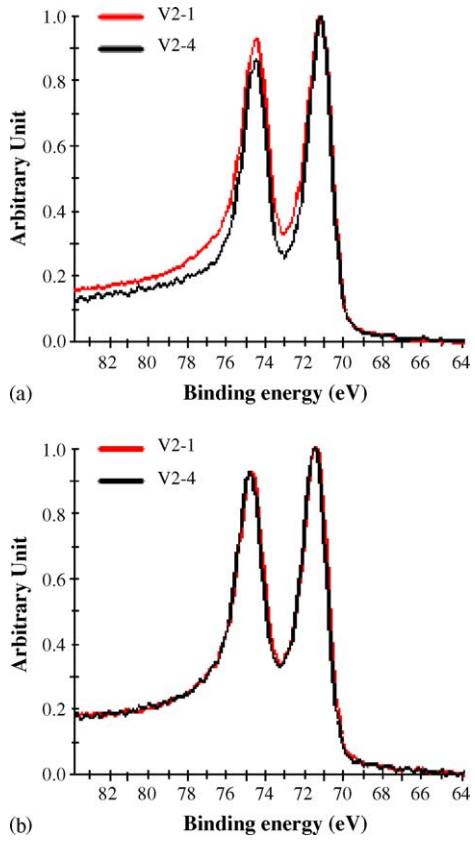

Fig. 8. XPS spectra of Pt 4f of each electrode: (a) cathode catalysts of V2-1 and V2-4 after the operation and (b) anode catalysts of V2-1 and V2-4 after the operation.

on the anode side (Fig. 8b). The result was thought to be in good agreement with the impedance data, which suggested primarily the deterioration of the cathode components.

4. Conclusion

A new approach in analyzing deteriorated MEAs by electrochemical impedance analysis and by physicochemical investigations, in combination, has been studied comprehensively. Separating the impedance values for the cathode and anode, a partial degradation of the cathode component due to a long-term continuous operation of 1000 h, is proposed. To clarify the relationship between the electrochemical properties and real MEA deteriorations, physicochemical investigations of the GDLs, MPLs and the catalyst layers were made. From the observed decrease of the GDL contact angle, morphology alteration and redistribution of the fluorinated water proofing agent in the GDLs and MPLs on cathode side, a resistance to mass transport has been identified. Furthermore, catalyst agglomeration in the densely packed catalyst layer and partial reduction of the catalyst could explain a decreased catalytic efficiency.

References

[1] S.D. Knights, K.M. Colbow, St. Pierre, D.P. Wilkinson, J. Power Sources 127 (2004) 127–134.
[2] C. Lim, C.Y. Wang, Electrochim. Acta 49 (2004) 4149–4156.
[3] M. Schulze, T. Knori, A. Schneider, E. Gulzow, J. Power Sources 127 (2004) 222–229.
[4] M. Schulze, A. Schneider, E. Gulzow, J. Power Sources 127 (2004) 213–221.
[5] D.A. Blom, J.R. Dunlap, T.A. Nolan, L.F. Allard, J. Electrochem. Soc. 150 (2003) A414–A418.
[6] M. Parasana, H.Y. Ha, E.A. Cho, S.A. Hong, I.H. Oh, J. Power Sources 131 (2004) 147–154.
[7] C.S. Kong, D.Y. Kim, H.K. Lee, Y.G. Shul, T.H. Lee, J. Power Sources 108 (2002) 185–191.
[8] H.S. Chu, C.Y. Yeh, F. Chen, J. Power Sources 123 (2003) 1–9.
[9] J.S. Lee, K.I. Han, S.O. Park, H.N. Kim, H. Kim, Electrochim. Acta 50 (2004) 807–810.
[10] T. Romero-Castanon, L.G. Arriaga, Y. Cano-Castillo, J. Power Sources 118 (2003) 179–182.
[11] J.T. Mueller, P.M. Urban, J. Power Sources 75 (1998) 139–143.
[12] A.S. Arico, P. Creti, P.L. Antonucci, J. Cho, H. Kim, V. Antonucci, Electrochim. Acta 24 (1998) 3719–3729.
[13] C. Huang, K.S. Tan, J. Lin, K.L. Tan, Chem. Phys. Lett. 371 (2003) 80–85.
[14] R.R. Diaz-Morales, R. Liu, E. Fachini, G. Chen, C.U. Serge, A. Martinez, C. Cabrera, E.S. Smotkin, J. Electrochem. Soc. 151 (2004) A1314–A1318.
[15] V. Alderucci, L. Pino, P.L. Antonucci, W. Roh, J. Cho, H. Kim, D.L. Cocke, V. Antonucci, Mater. Chem. Phys. 41 (1995) 9–14.